Supporting Information

Emergence of the novel magnetic properties in ternary iron nitrides toward spintronics: first-principles calculations

Ke Xiao,[a] Xiaohui Shi,[a,*] Xingyuan Zhang,[a] Qingming Ping,[a] Lulu Du[a,*]

[a]*School of Physics and Electronic Engineering, Linyi University, Linyi 276000, China*
Author to whom all correspondence should be addressed
[*]E-mail: shixiaohui@lyu.edu.cn;
[*]E-mail: dululu@lyu.edu.cn
† Electronic supplementary information (ESI) available.

S1. Valence electron configurations and *U* and *J* values of substitution atoms

Table S1 The valence–electron configurations of substitution atoms and the values of *U* and *J* used for the Y, Gd, W, and Pt atoms.

Atoms	Valence–electron	*U*(ev)	*J*(ev)
V	$4s^23d^3$	-	-
Cr	$4s^13d^5$	-	-
Mn	$4s^23d^5$	-	-
Fe	$4s^23d^6$	-	-
Co	$4s^23d^7$	-	-
Cu	$4s^13d^{10}$	-	-
Zn	$4s^23d^{10}$	-	-
Y	$5s^24d^1$	6.50	0
Gd	$4f^75d^1$	6.70	0
W	$4f^{14}5d^4$	3.93	0
Pt	$4f^{14}5d^9$	2.18	0

S2. Lattice constants of M^fFe_3N and M_3Fe^fN in the *a* and *c* axis

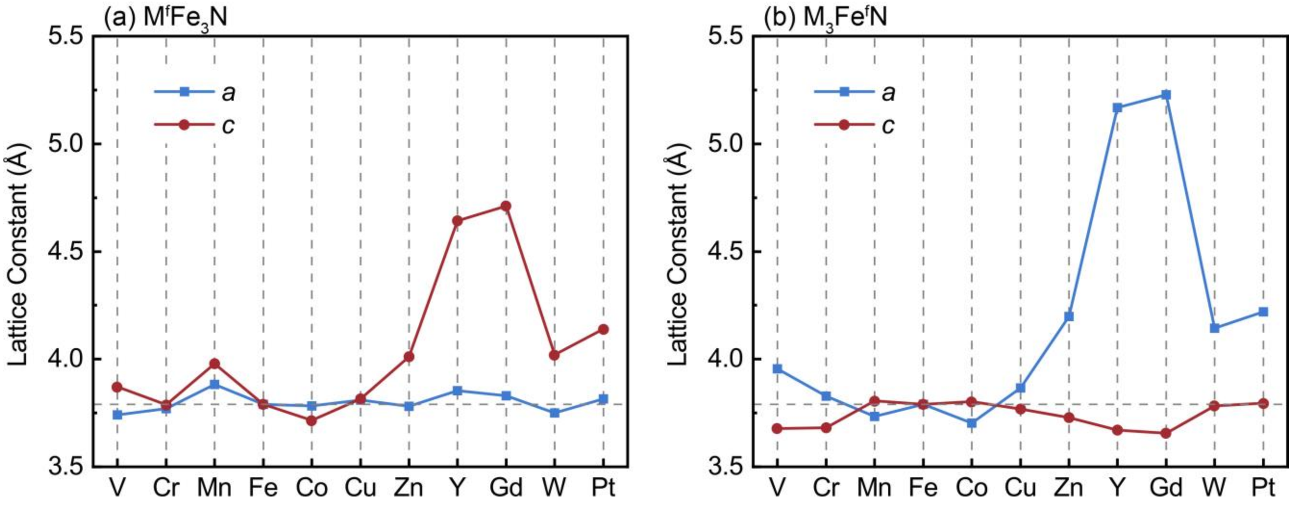

Figure S1 The lattice constants of (a) M^fFe_3N and (b) M_3Fe^fN, where the lattice constants of *a* and *c* are marked as blue and red point.

The *a*-axis of M^fFe_3N exhibits minor expansion when *M* are Y and Gd elements because the substitution of Fe_{IIB} sites not only change the *c*-axis lattice but also affect the bond lengths of the surrounding atoms. The change of bond lengths causes the *a*-axis expanding to accommodate the volume changes associated with the substitution elements. Compared to M^fFe_3N, the local environment is significantly changed in M_3Fe^fN. Possible reason is the substitution of multiple Fe atoms lead to a rearrangement of the overall lattice structure, which causes the *c*-axis to contract and achieves structural stabilization.

S3. Charge density difference of system Fe_4N

Table S2 Charge transfer situation of atoms at different sites of $M_xFe_{4-x}N$

	N (electrons /atom)	M_{IIAa} (electrons /atom)	M_{IIAb} (electrons /atom)	M_{IIB} (electrons /atom)	M_I (electrons /atom)
Fe_4N	1.33	-0.38	-0.38	-0.38	-0.18
Y^cFe_3N	1.42	0.10	0.10	0.10	-1.71
Y_3Fe^fN	1.56	-1.19	-1.19	1.17	-0.36
Gd_3Fe^cN	1.81	-1.11	-1.11	-1.11	1.52
Gd_3Fe^fN	1.42	-0.81	-0.81	0.33	-0.14
W_3Fe^fN	1.69	-0.68	-0.68	-0.13	-0.19

S4. Total DOS of $M_xFe_{4-x}N$ (M = V, Cr, Mn, Co, Cu, and Zn)

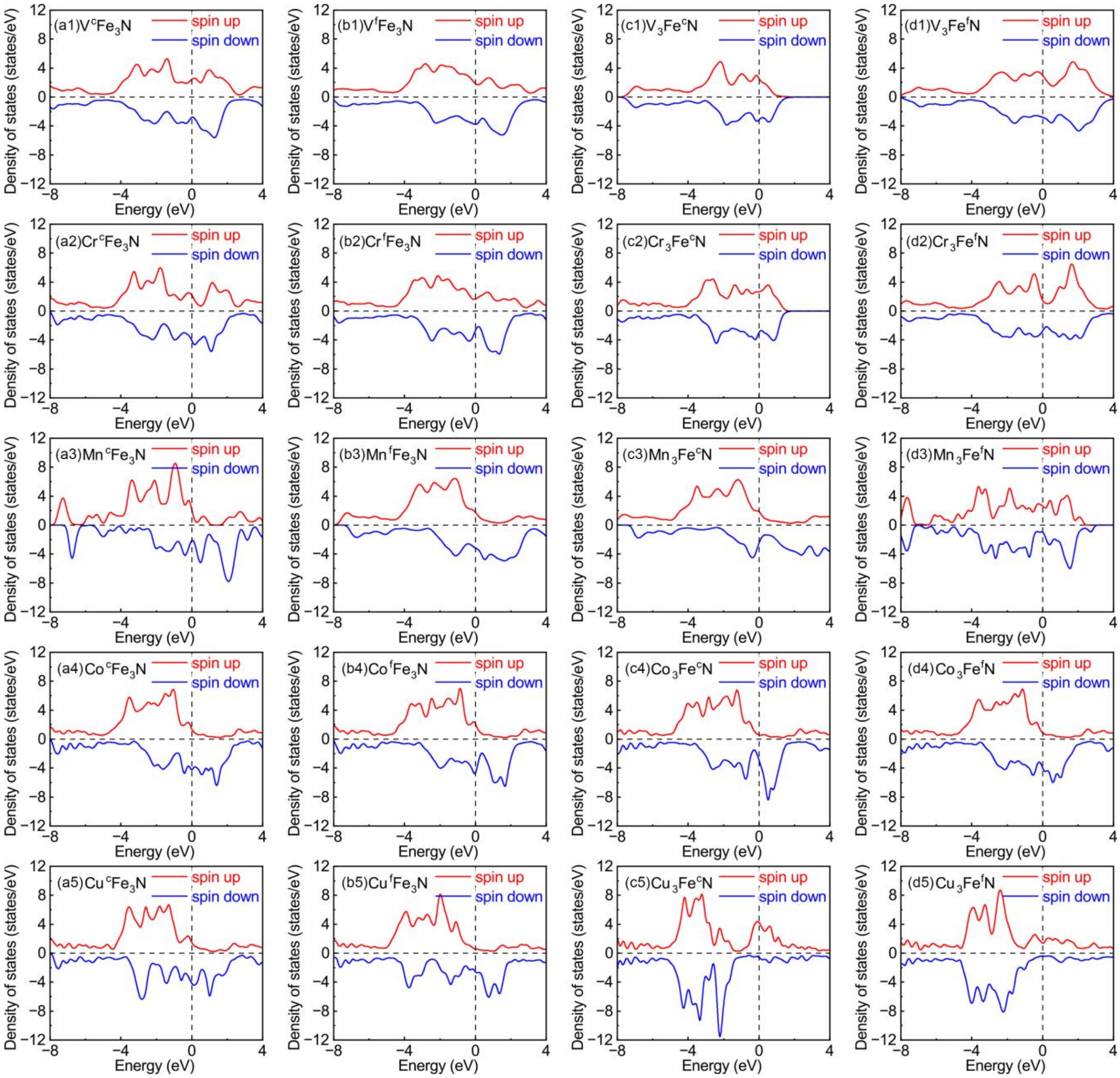

Figure S2 Total DOS of (a1-d1) $V_xFe_{4-x}N$, (a2-d2) $Cr_xFe_{4-x}N$, (a3-d3) $Mn_xFe_{4-x}N$, (a4-d4) $Co_xFe_{4-x}N$, and (a5-d5) $Cu_xFe_{4-x}N$ (x = 1 or 3).

S5. Total DOS of $M_xFe_{4-x}N$ (M = V, Zn, Y, Gd, W, and Pt)

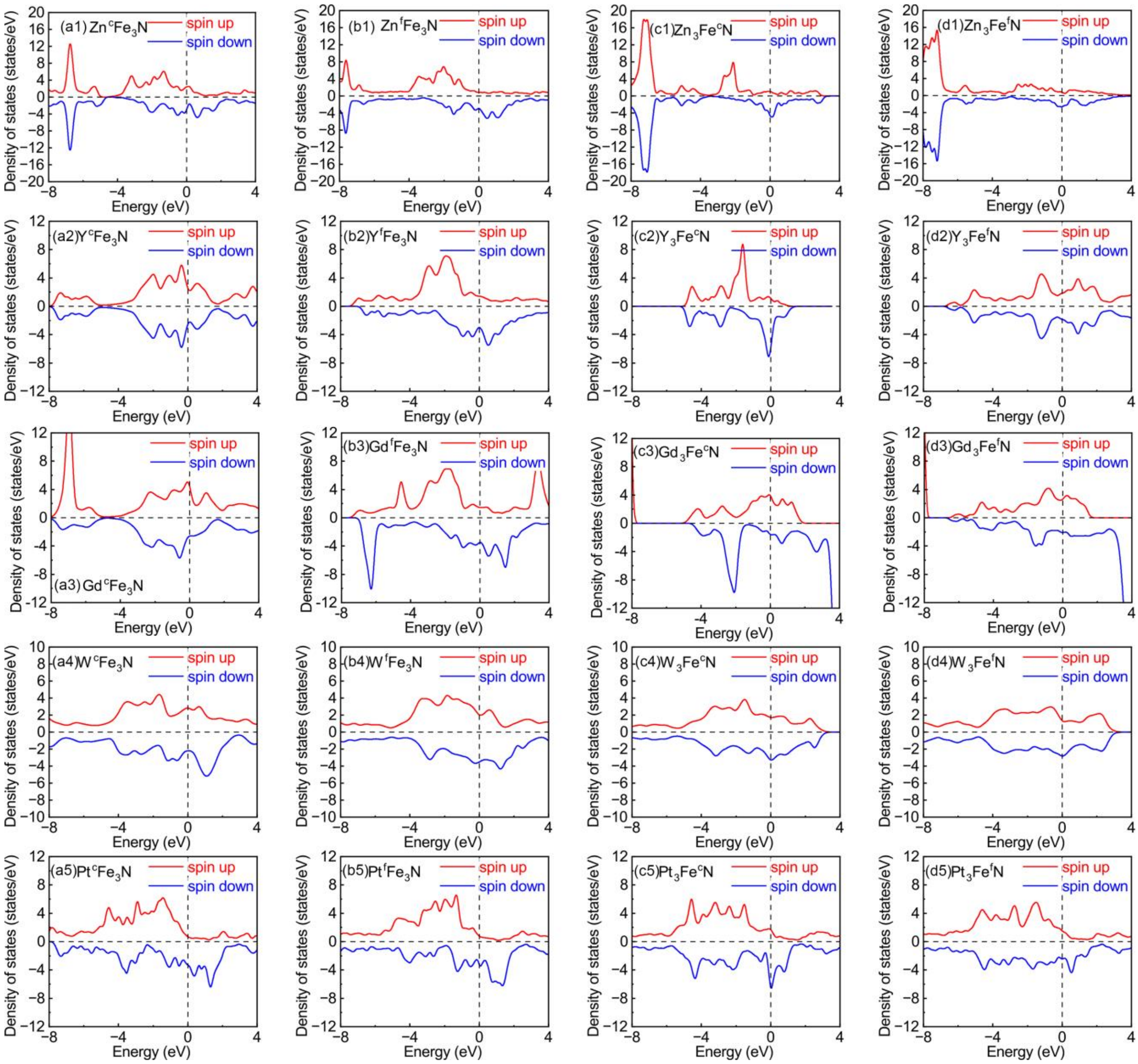

Figure S3 Total DOS of (a1-d1) $Zn_xFe_{4-x}N$, (a2-d2) $Y_xFe_{4-x}N$, (a3-d3) $Gd_xFe_{4-x}N$, (a4-d4) $W_xFe_{4-x}N$, and (a5-d5) $Pt_xFe_{4-x}N$ (x = 1 or 3).

S6. Total DOS, the atom-, orbital-resolved DOS of Fe_4N and $Pt_xFe_{4-x}N$ (x =1, or 3)

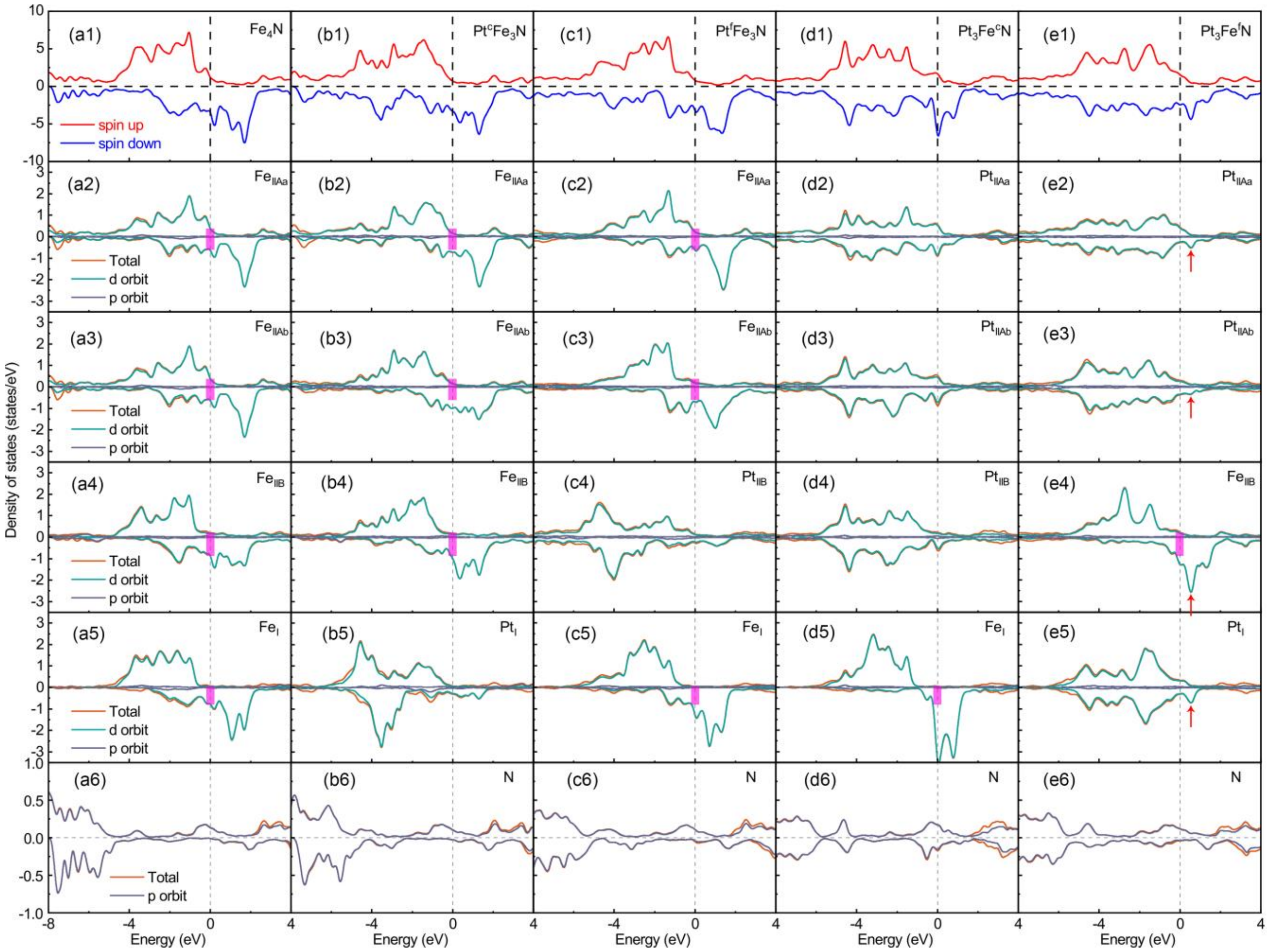

Figure S4 The total DOS of (a1) Fe_4N, (b1) Pt^cFe_3N, (c1) Pt^fFe_3N, (d1) Pt_3Fe^cN, and (e1) Pt_3Fe^fN. The atom-, *d*-orbit- and *p*- orbital-resolved DOS of (a2-e2) Fe_{IIAa}, (a3-e3) Fe_{IIAb}, (a4-e4) Fe_{IIB}, (a5-e5) Fe_I, and (a6-e6) N sites.

S7. Total DOS, the atom-, orbital-resolved DOS of Fe_4N and $Cu_xFe_{4-x}N$ (x =1, or 3)

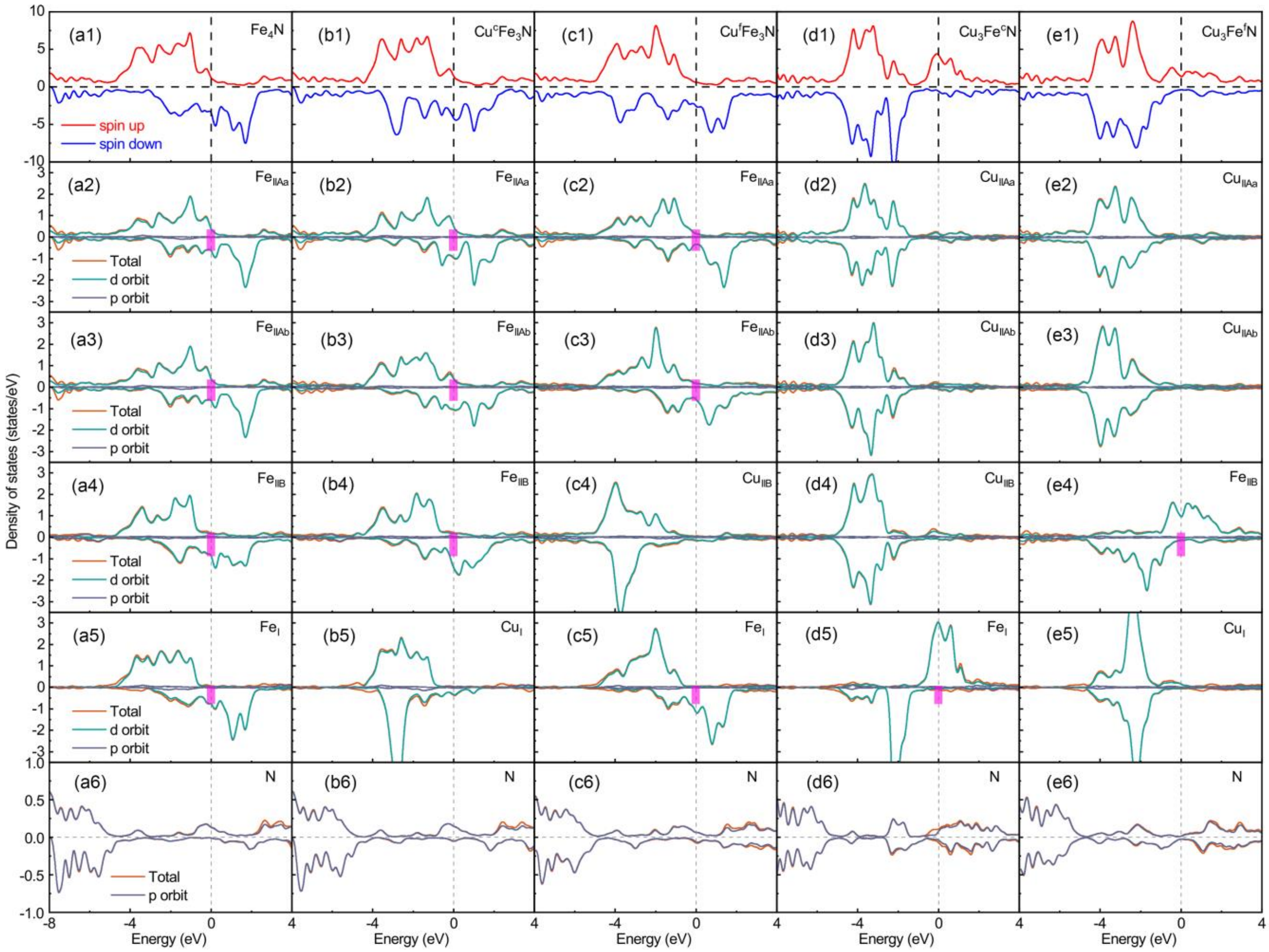

Figure S5 The total DOS of (a1) Fe_4N, (b1) Cu^cFe_3N, (c1) Cu^fFe_3N, (d1) Cu_3Fe^cN, and (e1) Cu_3Fe^fN. The atom-, *d*-orbit- and *p*- orbital-resolved DOS of (a2-e2) Fe_{IIAa}, (a3-e3) Fe_{IIAb}, (a4-e4) Fe_{IIB}, (a5-e5) Fe_I, and (a6-e6) N sites.

S8. Total DOS, the atom-, orbital-resolved DOS of Fe_4N and $Zn_xFe_{4-x}N$ (x =1, or 3)

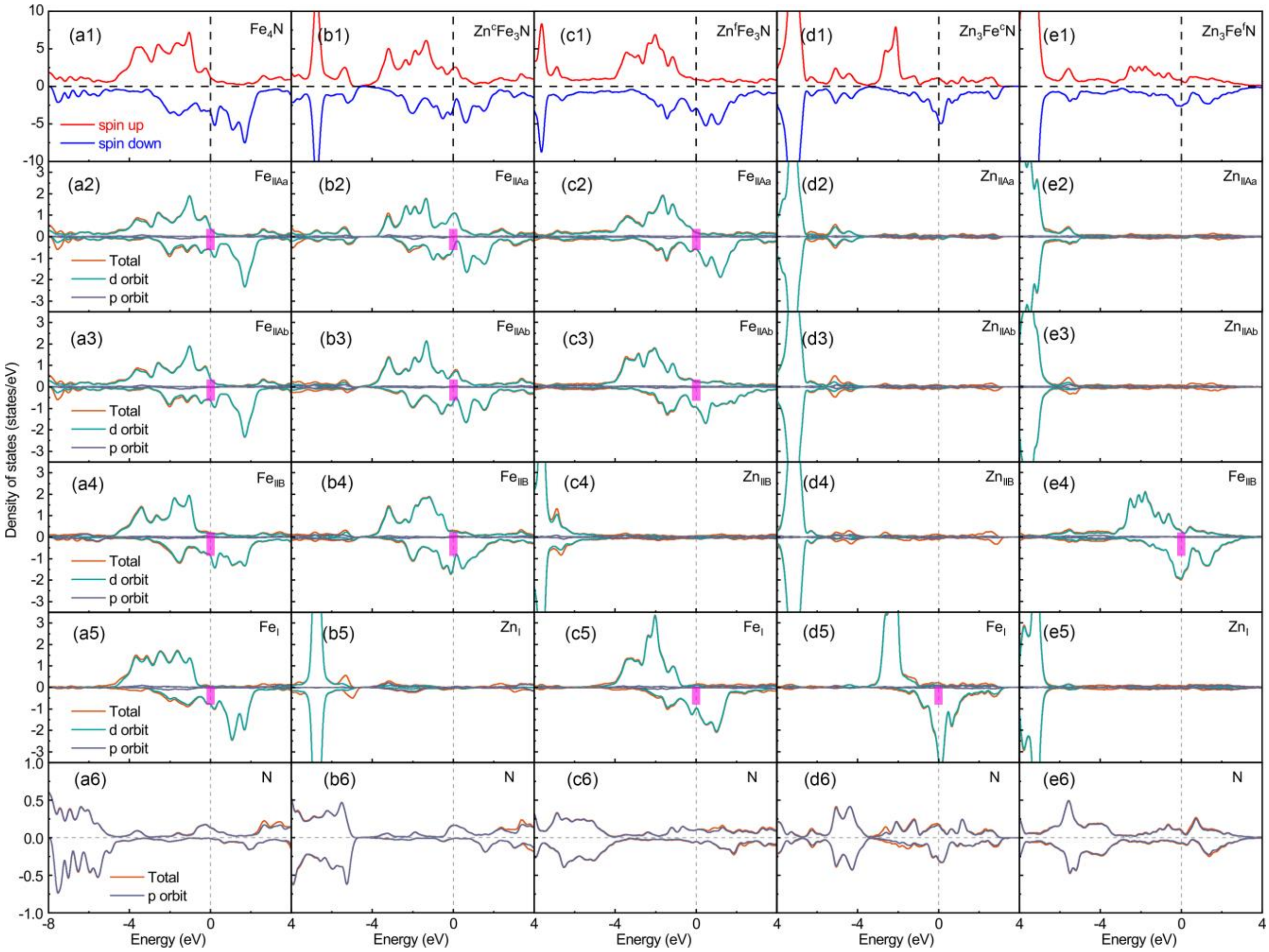

Figure S6 The total DOS of (a1) Fe_4N, (b1) Zn^cFe_3N, (c1) Zn^fFe_3N, (d1) Zn_3Fe^cN, and (e1) Zn_3Fe^fN. The atom-, *d*-orbit- and *p*- orbital-resolved DOS of (a2-e2) Fe_{IIAa}, (a3-e3) Fe_{IIAb}, (a4-e4) Fe_{IIB}, (a5-e5) Fe_I, and (a6-e6) N sites.

S9. Total DOS, the atom-, orbital-resolved DOS of Fe_4N and $Co_xFe_{4-x}N$ (x =1, or 3)

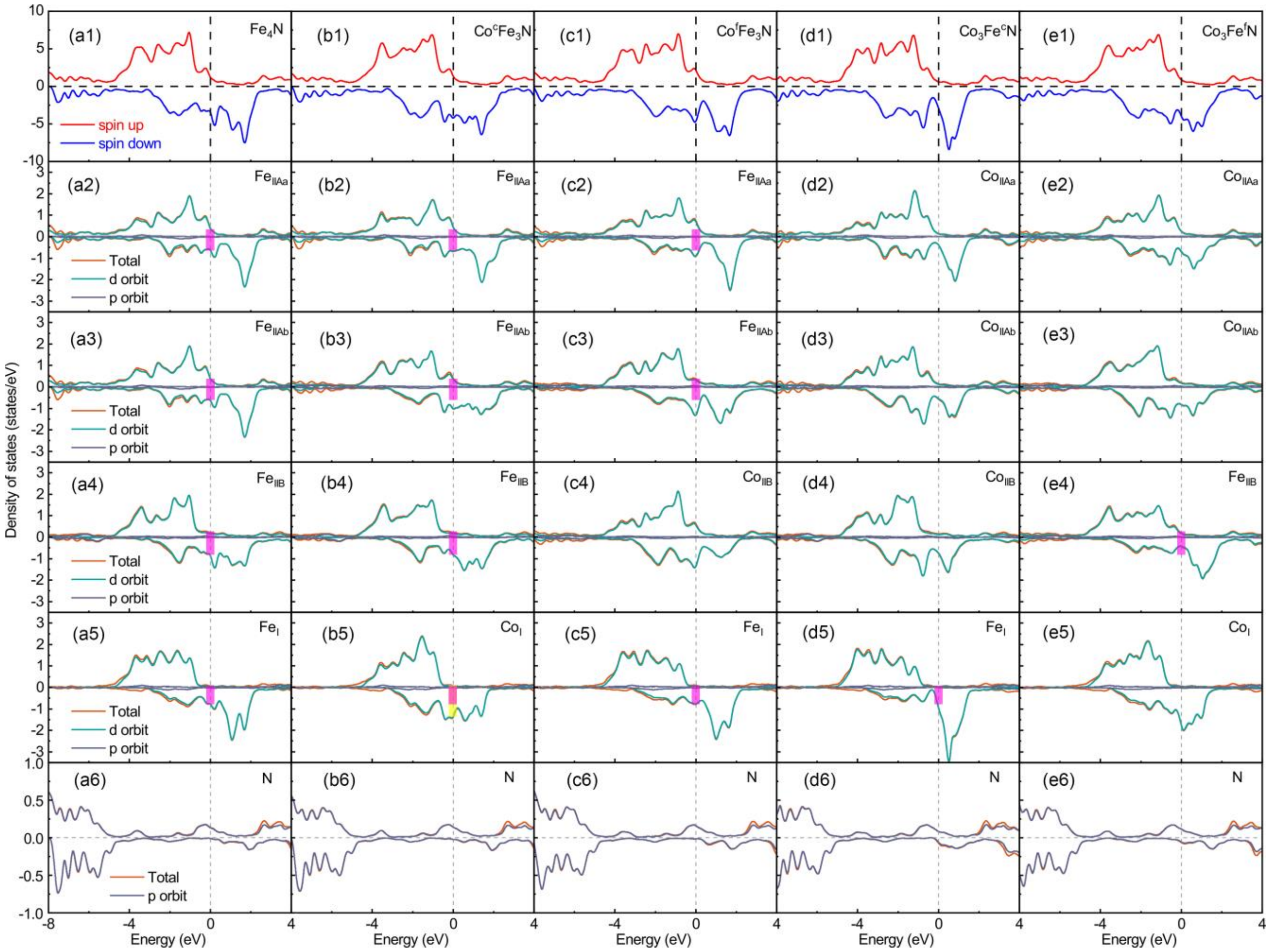

Figure S7 The total DOS of (a1) Fe_4N, (b1) Co^cFe_3N, (c1) Co^fFe_3N, (d1) Co_3Fe^cN, and (e1) Co_3Fe^fN. The atom-, *d*-orbit- and *p*- orbital-resolved DOS of (a2-e2) Fe_{IIAa}, (a3-e3) Fe_{IIAb}, (a4-e4) Fe_{IIB}, (a5-e5) Fe_I, and (a6-e6) N sites.

S10. Total DOS, the atom-, orbital-resolved DOS of Fe_4N and $V_xFe_{4-x}N$ (x =1, or 3)

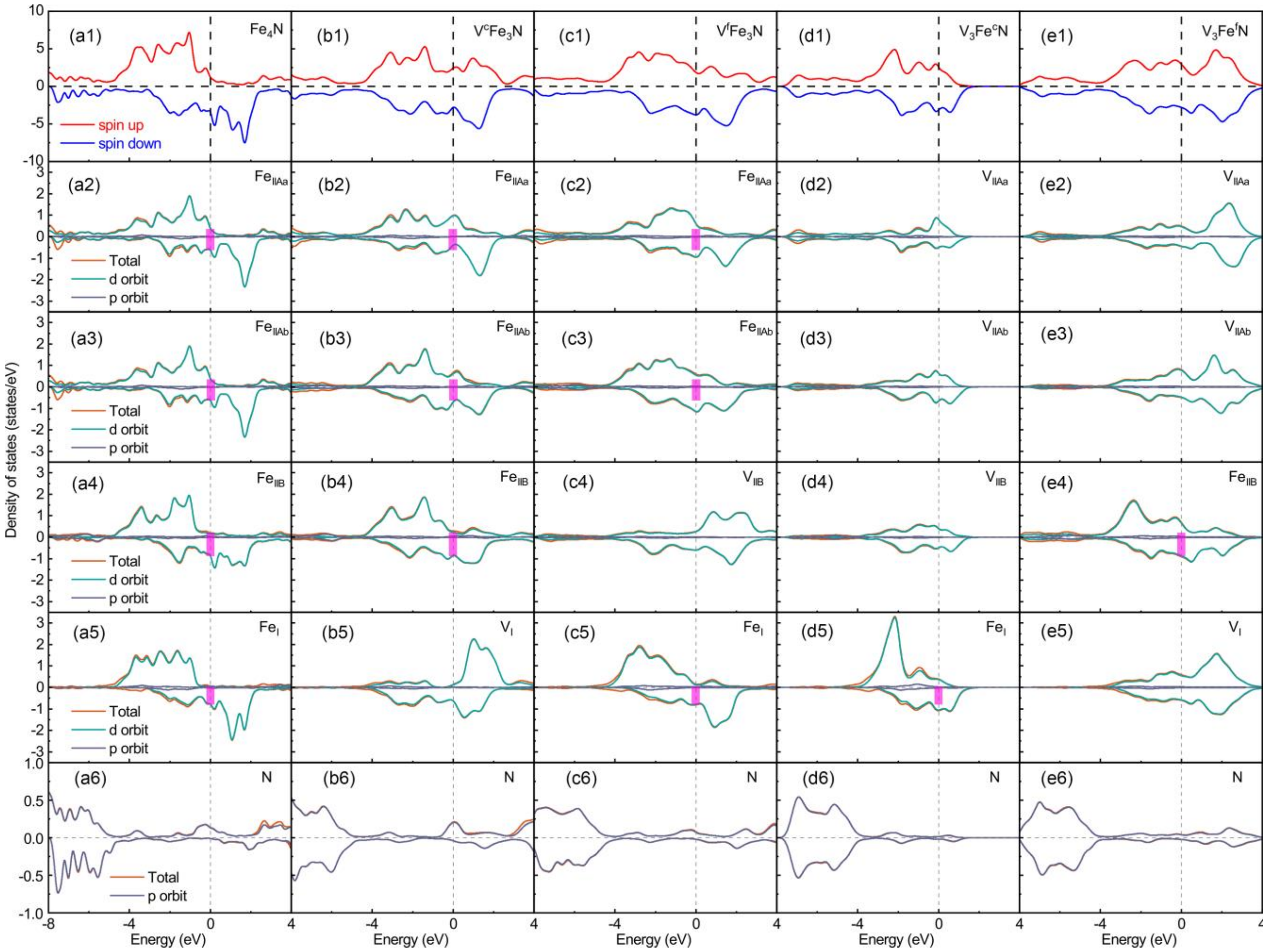

Figure S8 The total DOS of (a1) Fe_4N, (b1) V^cFe_3N, (c1) V^fFe_3N, (d1) V_3Fe^cN, and (e1) V_3Fe^fN. The atom-, *d*-orbit- and *p*- orbital-resolved DOS of (a2-e2) Fe_{IIAa}, (a3-e3) Fe_{IIAb}, (a4-e4) Fe_{IIB}, (a5-e5) Fe_I, and (a6-e6) N sites.

S11. Total DOS, the atom-, orbital-resolved DOS of Fe_4N and $Cr_xFe_{4-x}N$ (x =1, or 3)

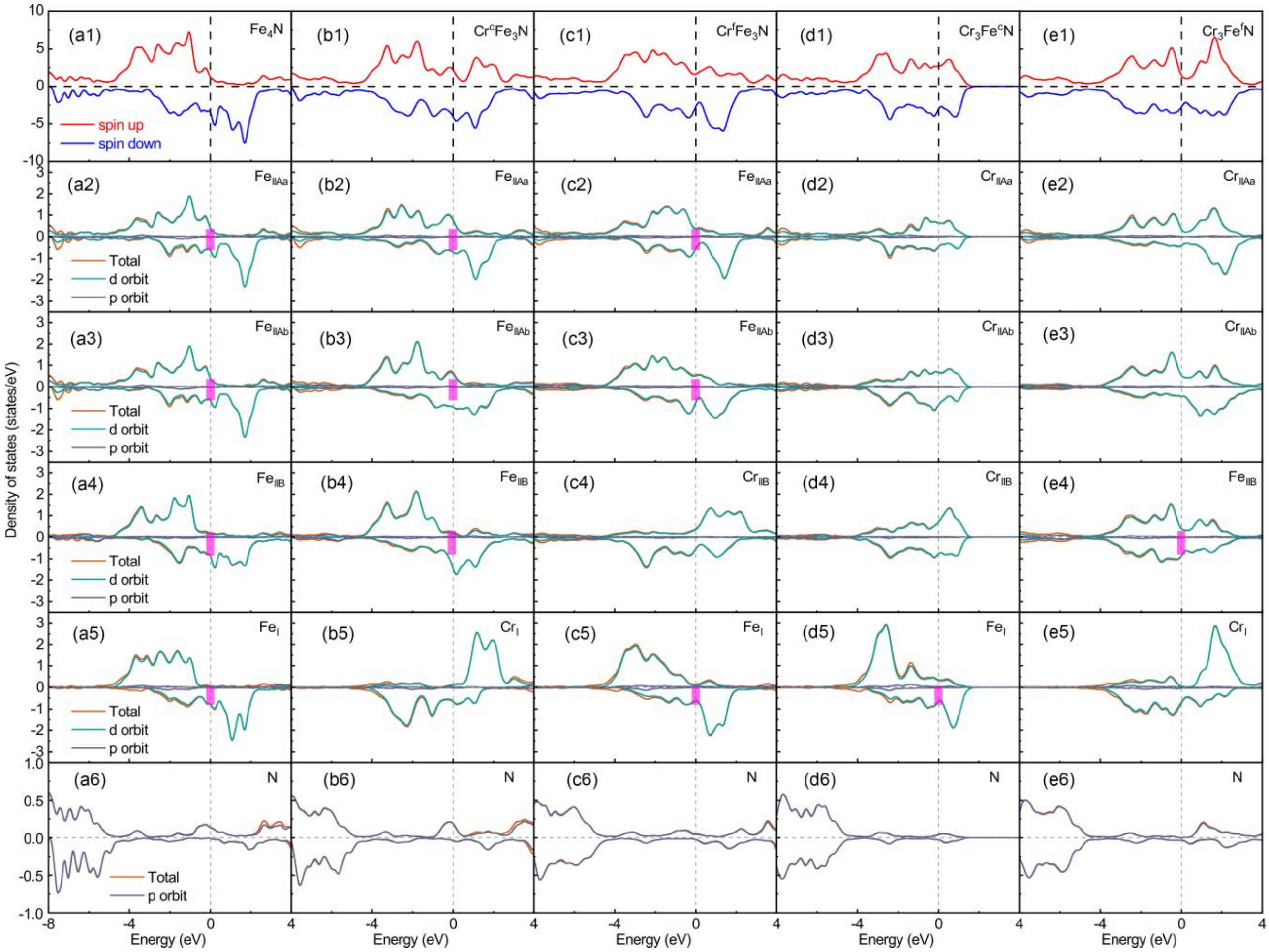

Figure S9 The total DOS of (a1) Fe_4N, (b1) Cr^cFe_3N, (c1) Cr^fFe_3N, (d1) Cr_3Fe^cN, and (e1) Cr_3Fe^fN. The atom-, *d*-orbit- and *p*- orbital-resolved DOS of (a2-e2) Fe_{IIAa}, (a3-e3) Fe_{IIAb}, (a4-e4) Fe_{IIB}, (a5-e5) Fe_I, and (a6-e6) N sites.

S12. Total DOS, the atom-, orbital-resolved DOS of Fe_4N and $Gd_xFe_{4-x}N$ (x =1, or 3)

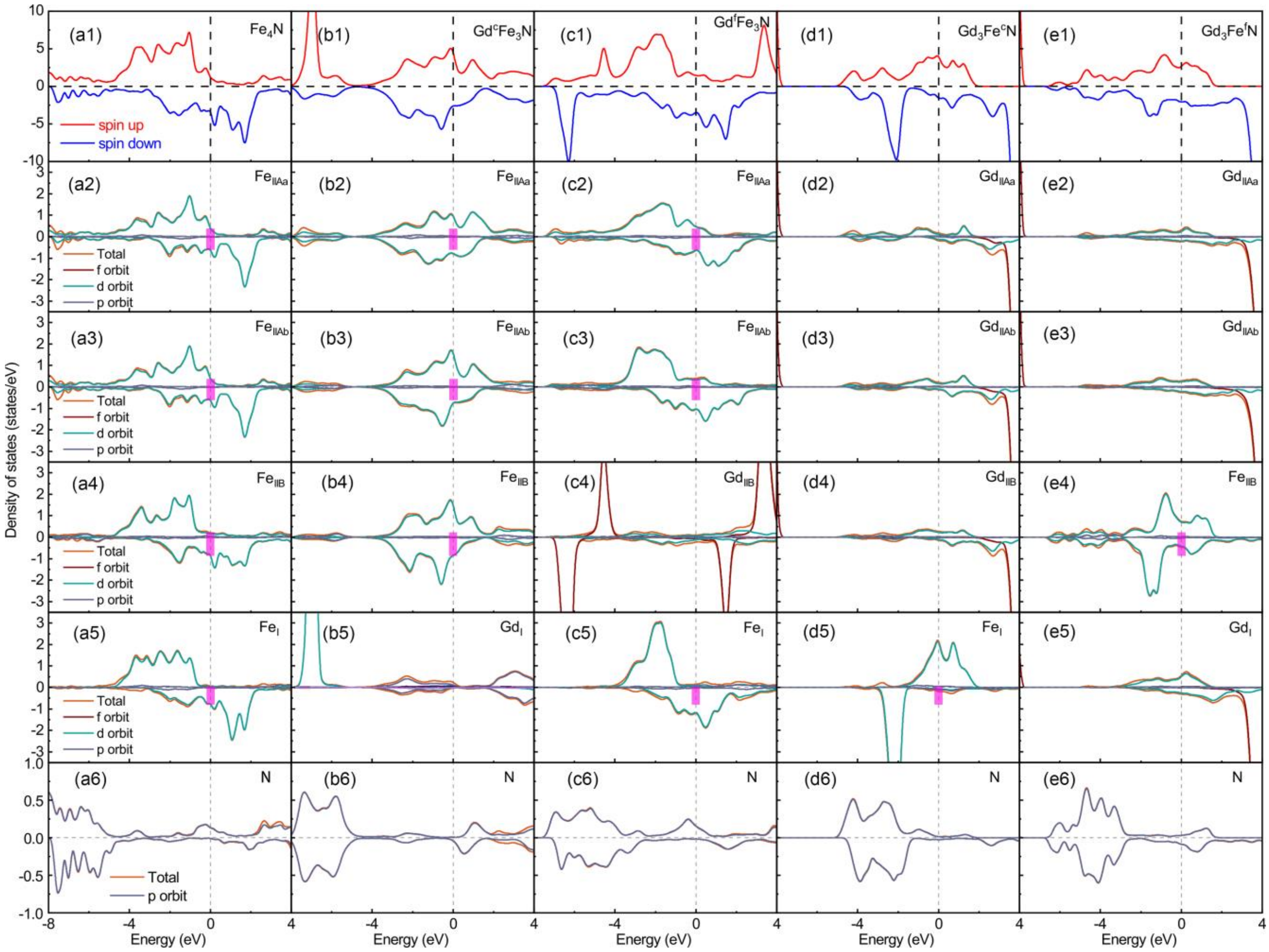

Figure S10 The total DOS of (a1) Fe_4N, (b1) Gd^cFe_3N, (c1) Gd^fFe_3N, (d1) Gd_3Fe^cN, and (e1) Gd_3Fe^fN. The atom-, *d*-orbit- and *p*- orbital-resolved DOS of (a2-e2) Fe_{IIAa}, (a3-e3) Fe_{IIAb}, (a4-e4) Fe_{IIB}, (a5-e5) Fe_I, and (a6-e6) N sites.

S13. Total DOS, the atom-, orbital-resolved DOS of Fe_4N and $W_xFe_{4-x}N$ (x =1, or 3)

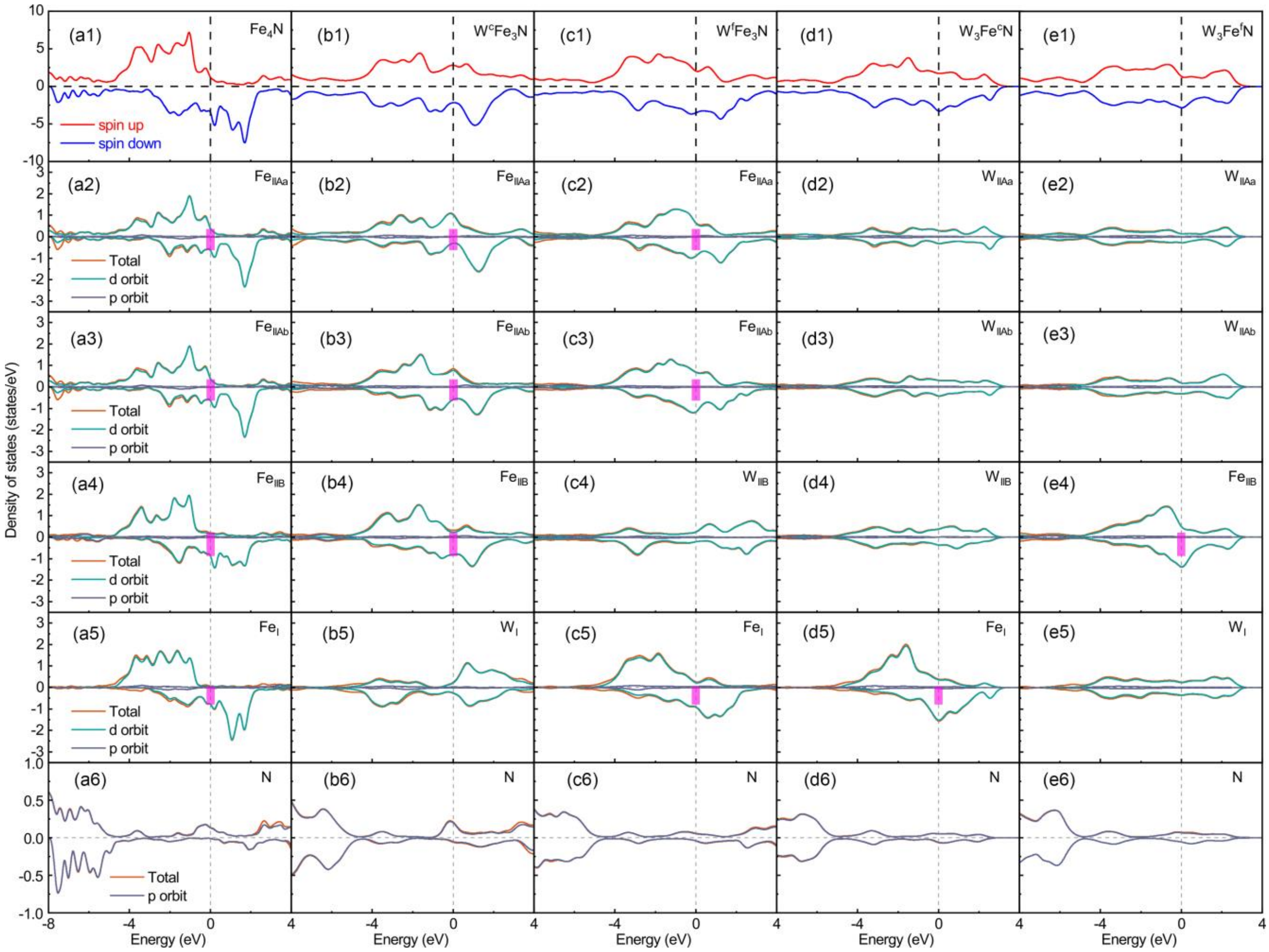

Figure S11 The total DOS of (a1) Fe_4N, (b1) W^cFe_3N, (c1) W^fFe_3N, (d1) W_3Fe^cN, and (e1) W_3Fe^fN. The atom-, *d*-orbit- and *p*- orbital-resolved DOS of (a2-e2) Fe_{IIAa}, (a3-e3) Fe_{IIAb}, (a4-e4) Fe_{IIB}, (a5-e5) Fe_I, and (a6-e6) N sites.

S14. Total DOS, the atom-, orbital-resolved DOS of Fe_4N and $Y_xFe_{4-x}N$ (x =1, or 3)

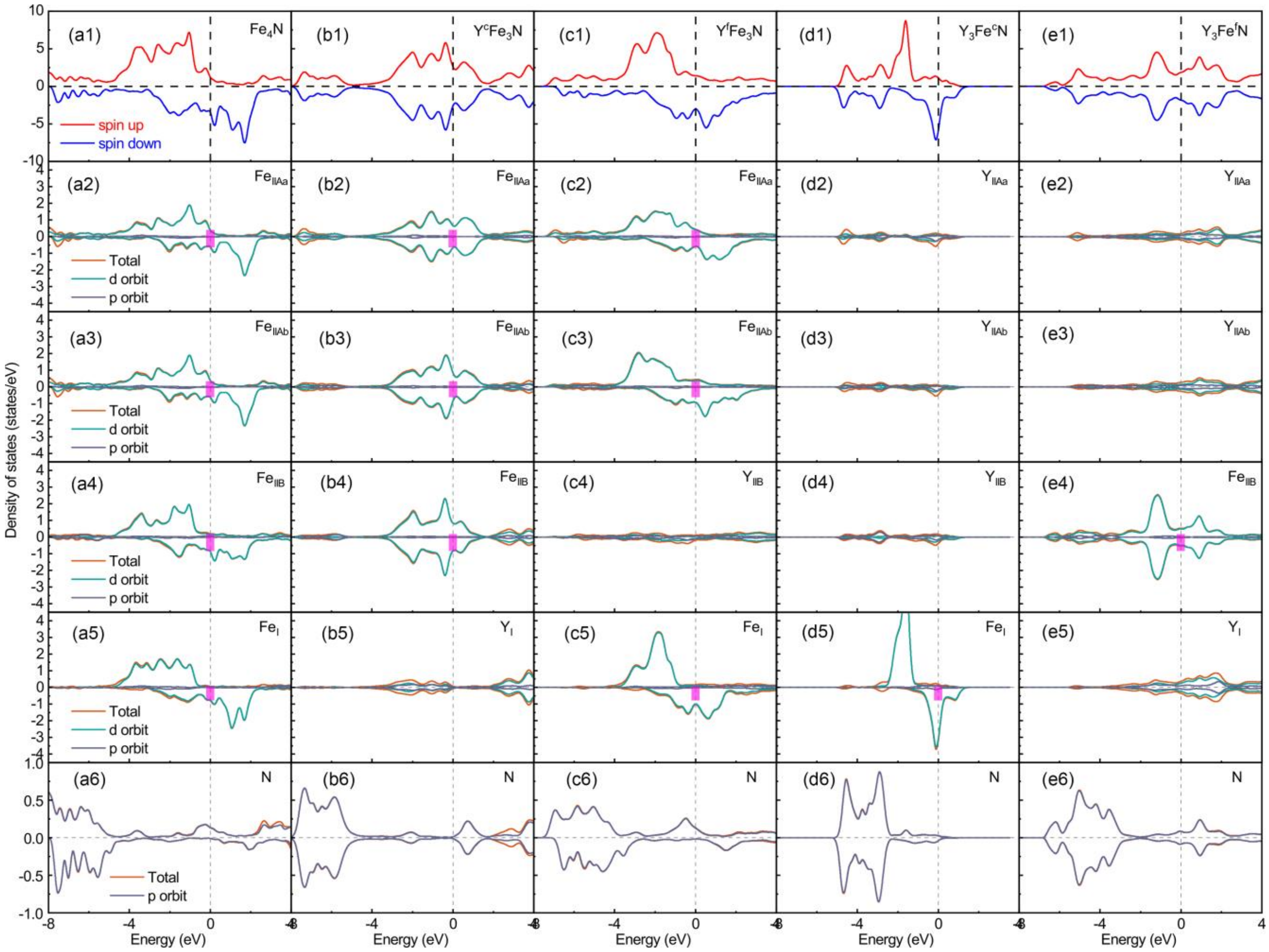

Figure S12 The total DOS of (a1) Fe_4N, (b1) Y^cFe_3N, (c1) Y^fFe_3N, (d1) Y_3Fe^cN, and (e1) Y_3Fe^fN. The atom-, *d*-orbit- and *p*- orbital-resolved DOS of (a2-e2) Fe_{IIAa}, (a3-e3) Fe_{IIAb}, (a4-e4) Fe_{IIB}, (a5-e5) Fe_I, and (a6-e6) N sites.

S15. Total DOS, the atom-, orbital-resolved DOS of Fe_4N and $Mn_xFe_{4-x}N$ (x =1, or 3)

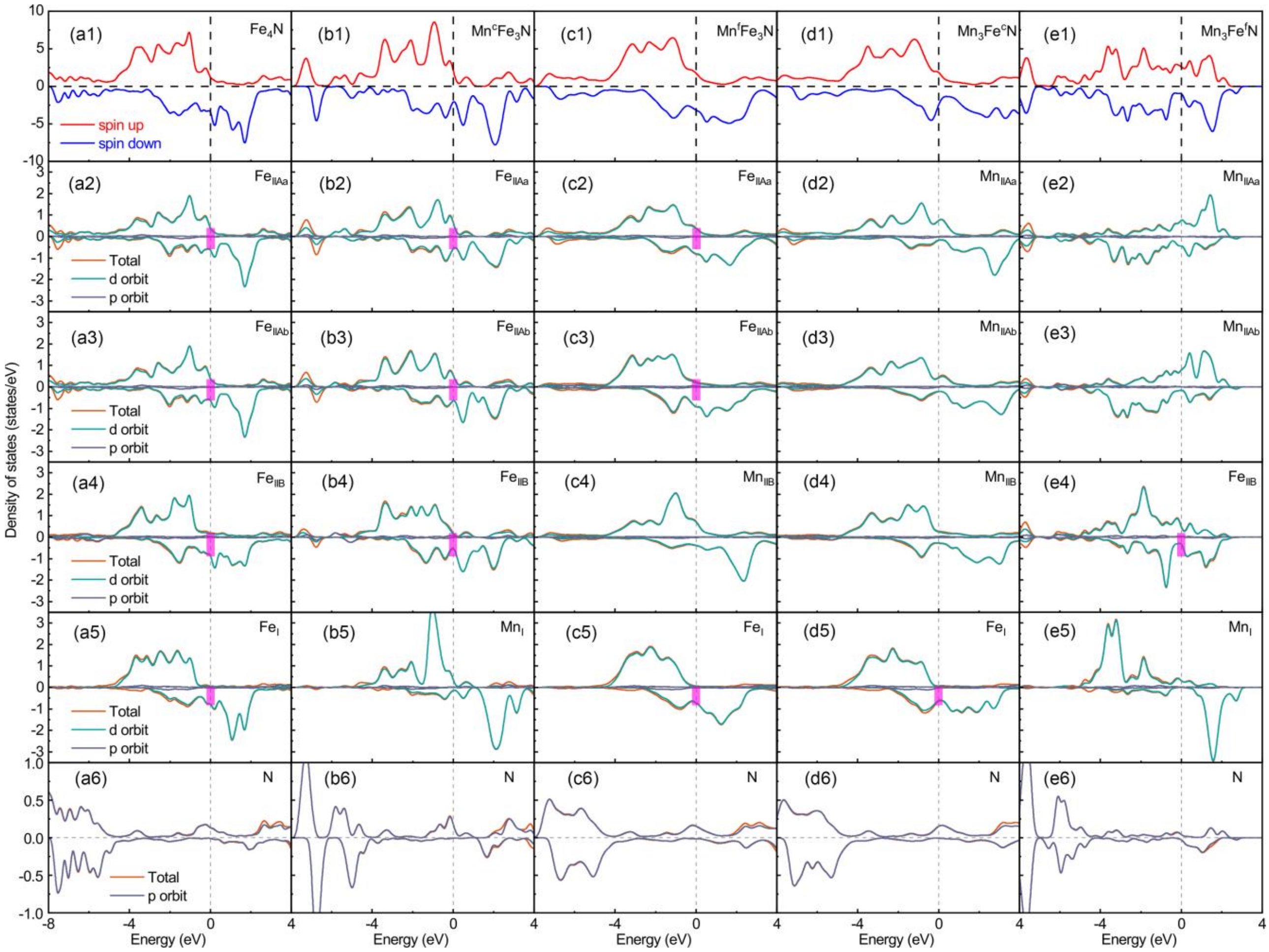

Figure S13 The total DOS of (a1) Fe_4N, (b1) Mn^cFe_3N, (c1) Mn^fFe_3N, (d1) Mn_3Fe^cN, and (e1) Mn_3Fe^fN. The atom-, *d*-orbit- and *p*- orbital-resolved DOS of (a2-e2) Fe_{IIAa}, (a3-e3) Fe_{IIAb}, (a4-e4) Fe_{IIB}, (a5-e5) Fe_I, and (a6-e6) N sites.

S16. The orbital-resolved MAE of Fe_4N and M_3Fe^fN (M = V, Cu, and Zn)

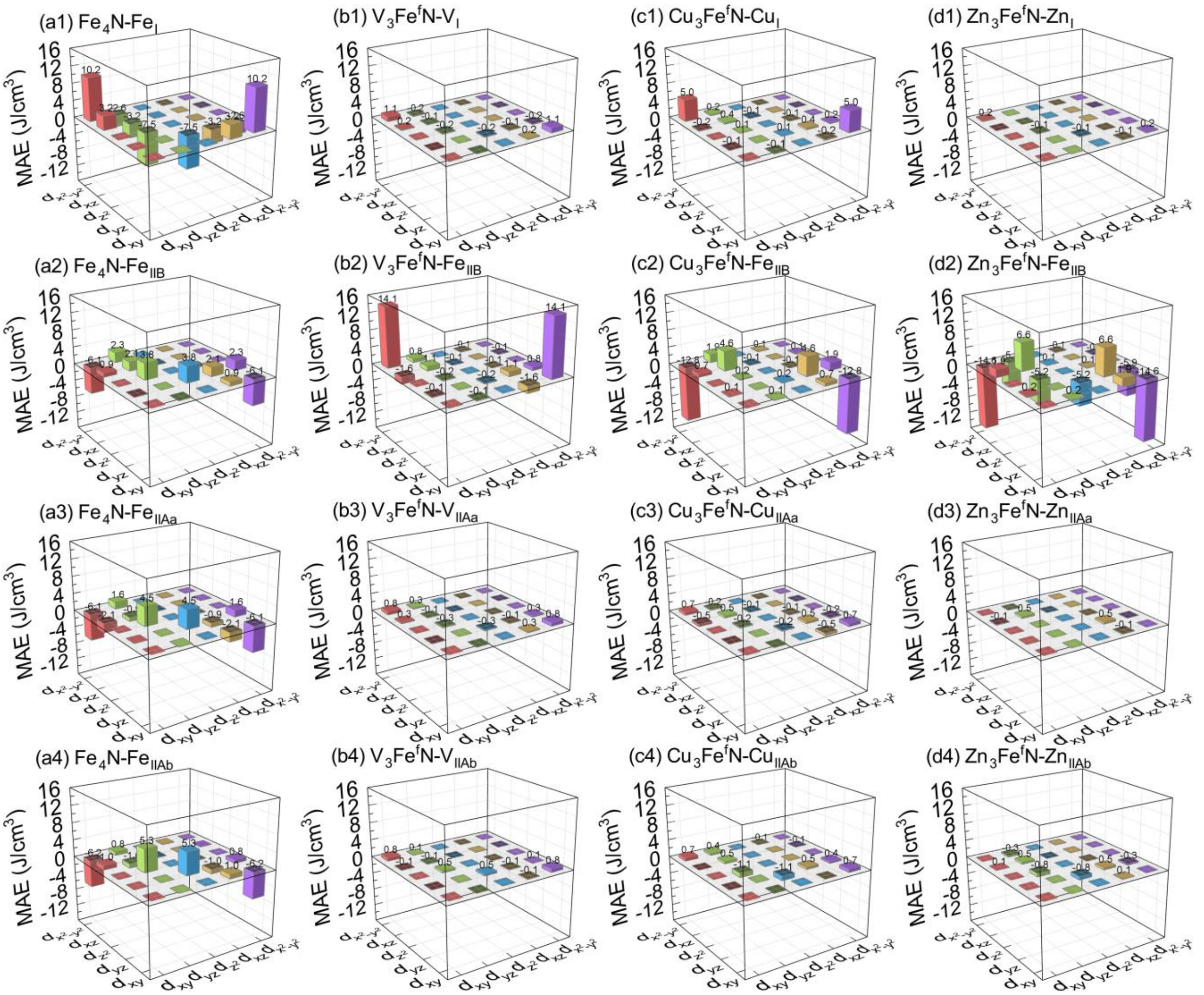

Figure S14 The orbital-resolved MAE of (a1-a4) Fe_4N, (b1-b4) V_3Fe^fN, (c1-c4) Cu_3Fe^fN, and (d1-d4) Zn^fFe_3N.

The orbital-resolved MAE of (a1-e1) Fe_I, (a2-e2) Fe_{IIB}, (a3-e3) Fe_{IIAa}, and (a4-e4) Fe_{IIAb} sites.

S17. The orbital-resolved MAE of Fe_4N and M^fFe_3N (M =Cr and Mn)

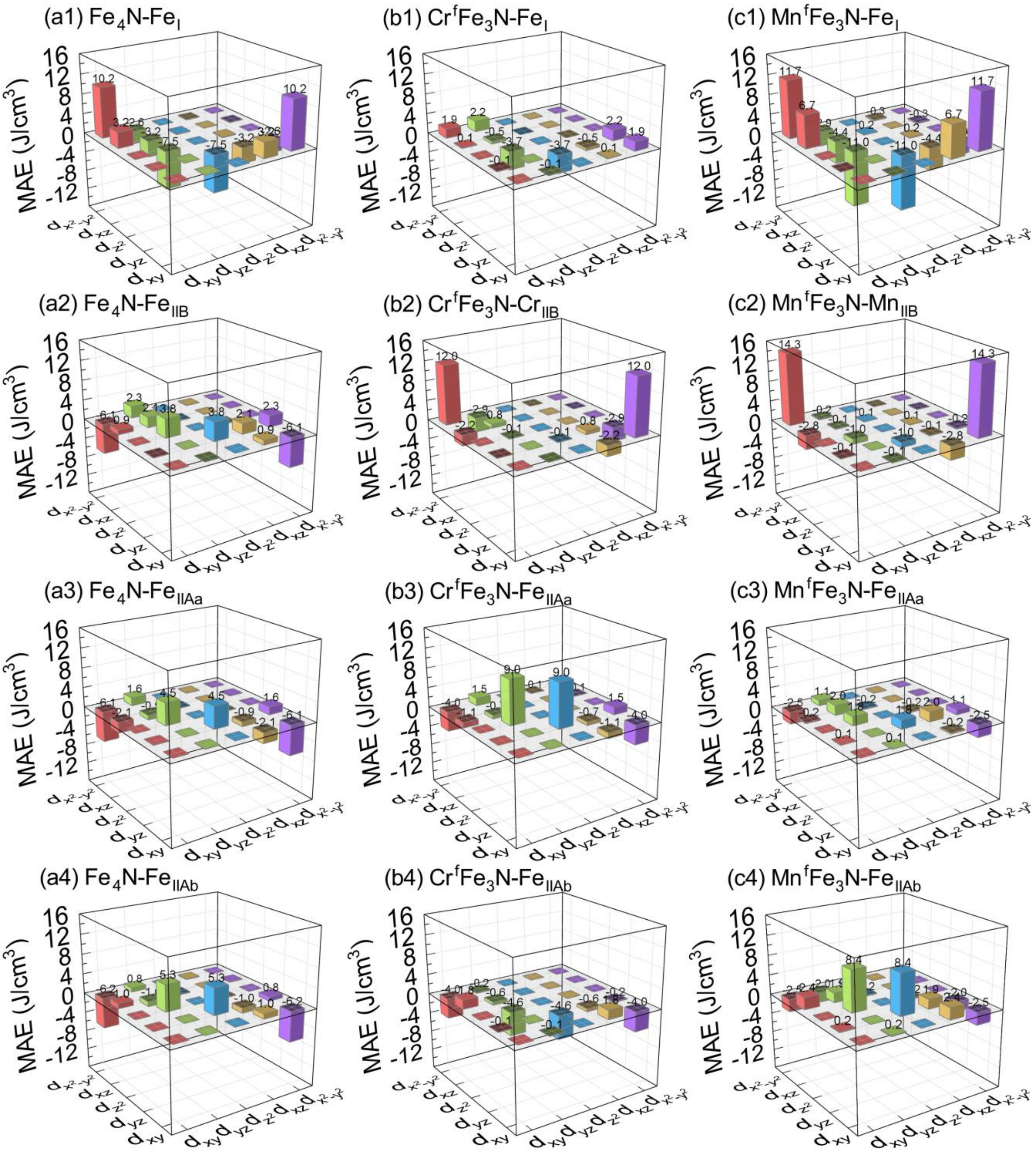

Figure S15 The orbital-resolved MAE of (a1-a4) Fe_4N, (b1-b4) Cr^fFe_3N, and (c1-c4) Mn^fFe_3N. The orbital-resolved MAE of (a1-c1) Fe_I, (a2-c2) Fe_{IIB}, (a3-c3) Fe_{IIAa}, and (a4-c4) Fe_{IIAb} sites.

S18. The orbital-resolved MAE of Fe_4N and M_3Fe^fN (M =Cr and Mn)

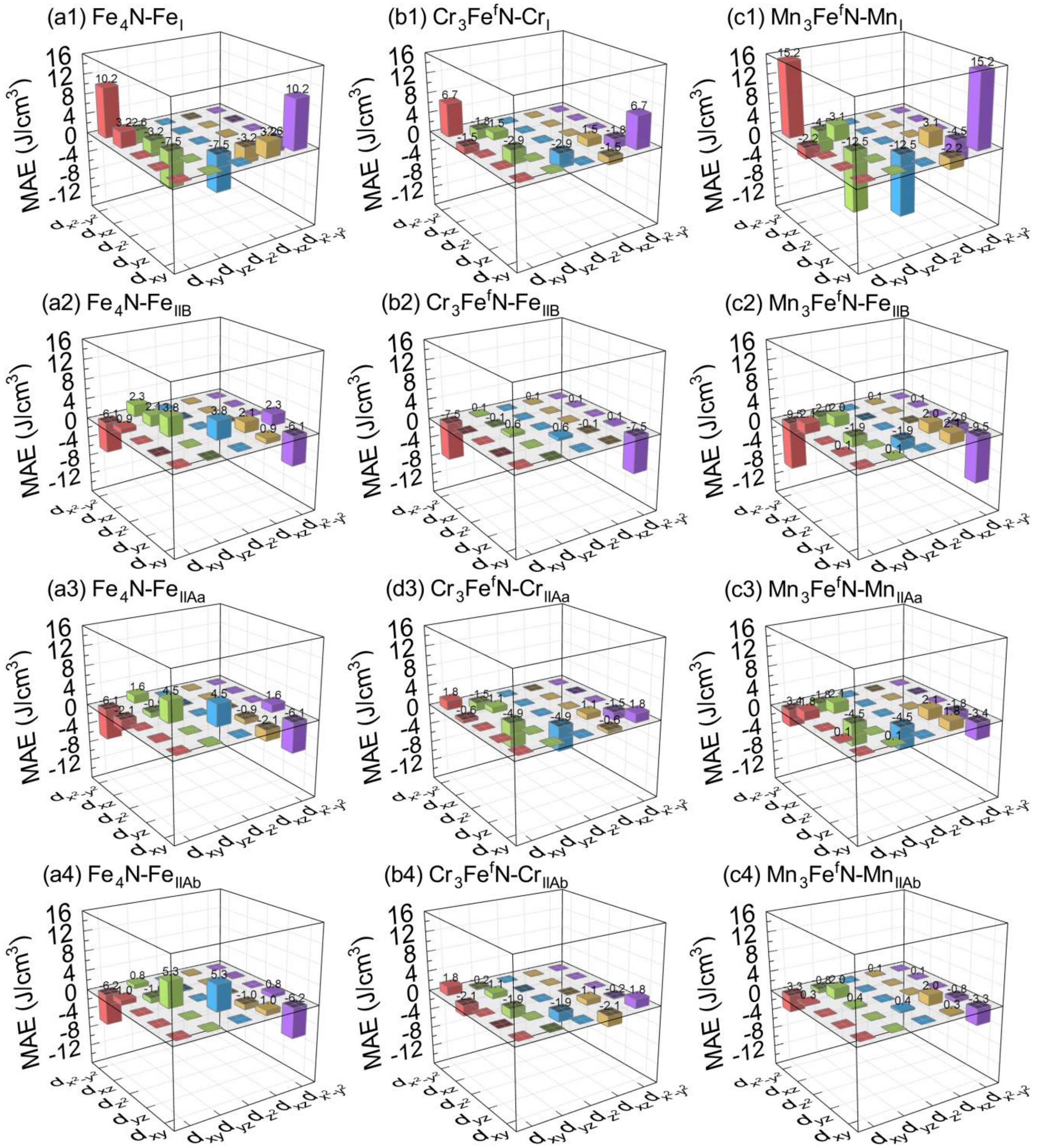

Figure S16 The orbital-resolved MAE of (a1-a4) Fe_4N, (b1-b4) Cr_3Fe^fN, and (c1-c4) Mn_3Fe^fN. The orbital-resolved MAE of (a1-c1) Fe_I, (a2-c2) Fe_{IIB}, (a3-c3) Fe_{IIAa}, and (a4-c4) Fe_{IIAb} sites.

S19. The orbital-resolved MAE of Fe_4N and M_3Fe^fN (*M* =Co and Gd)

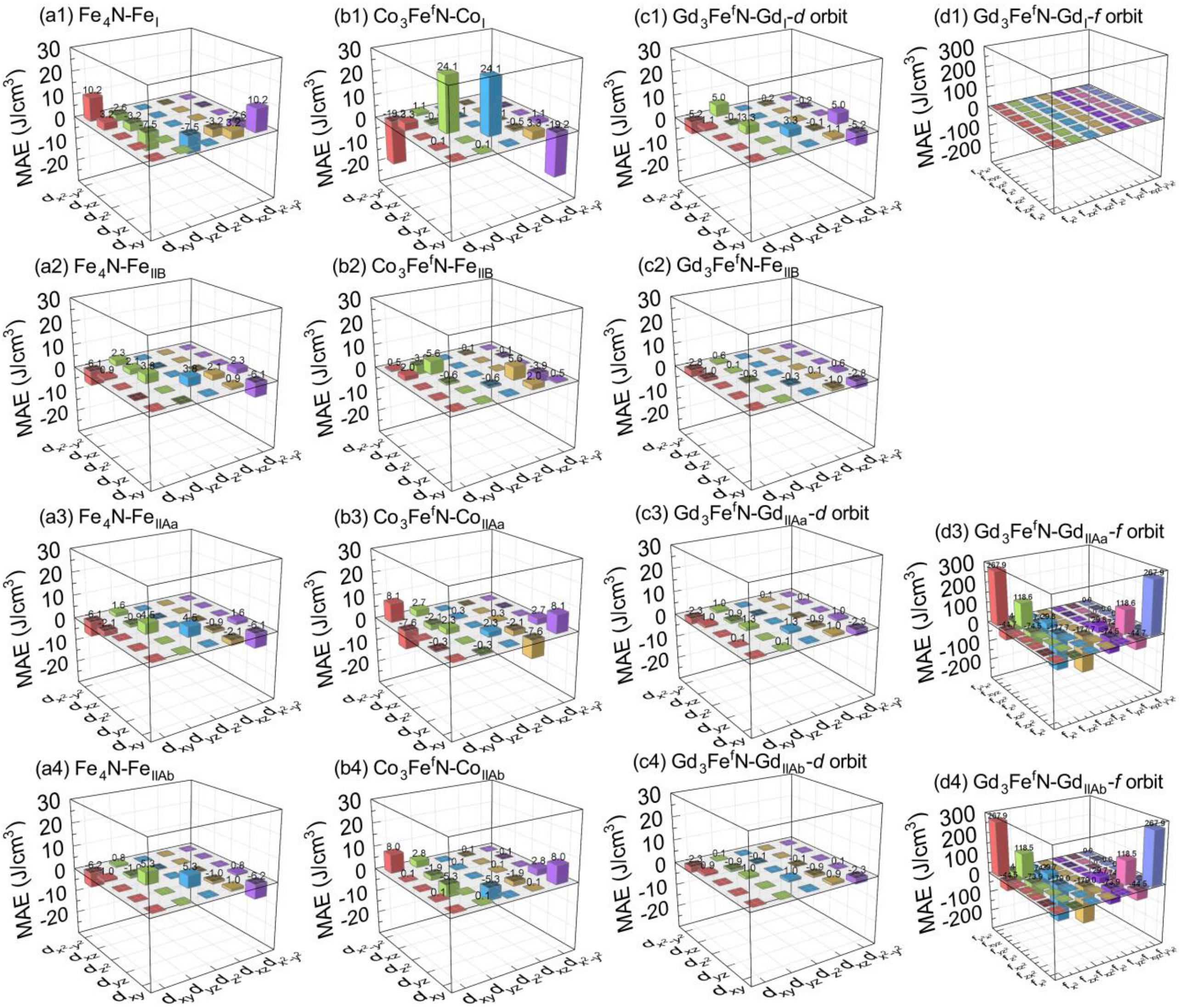

Figure S17 The orbital-resolved MAE of (a1-a4) Fe_4N, (b1-b4) Co_3Fe^fN, and (c1-c4) Gd_3Fe^fN. The orbital-resolved MAE of (a1-d1) Fe_I, (a2-c2) Fe_{IIB}, (a3-d3) Fe_{IIAa}, and (a4-d4) Fe_{IIAb} sites.

S20. The orbital-resolved MAE of Fe_4N and M^fFe_3N (M =Co and Gd)

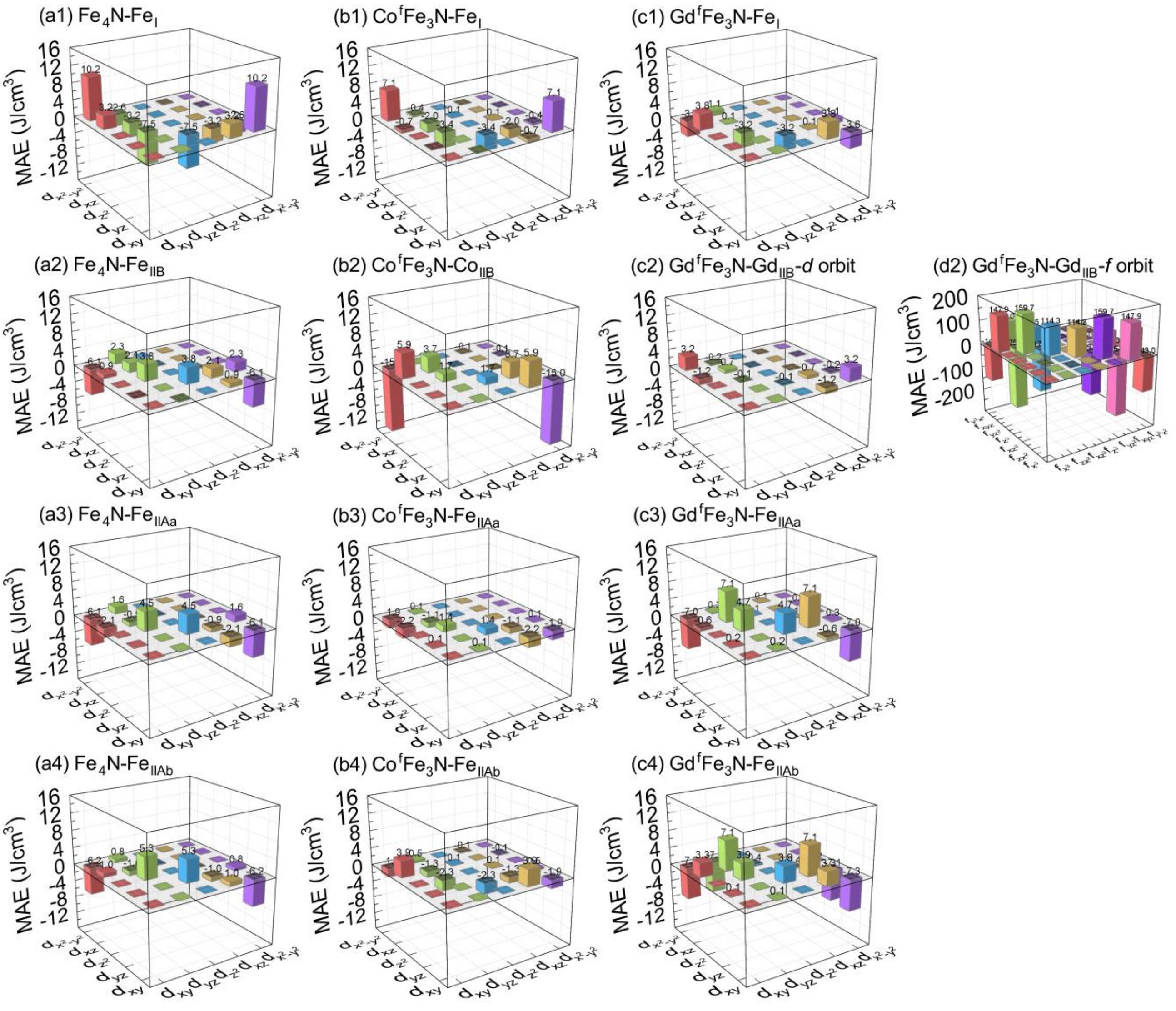

Figure S18 The orbital-resolved MAE of (a1-a4) Fe_4N, (b1-b4) Co^fFe_3N, and (c1-c4) Gd^fFe_3N. The orbital-resolved MAE of (a1-c1) Fe_I, (a2-d2) Fe_{IIB}, (a3-c3) Fe_{IIAa}, and (a4-c4) Fe_{IIAb} sites sites.

S21. The orbital-resolved MAE of Fe_4N and M^fFe_3N (*M* =W and Pt)

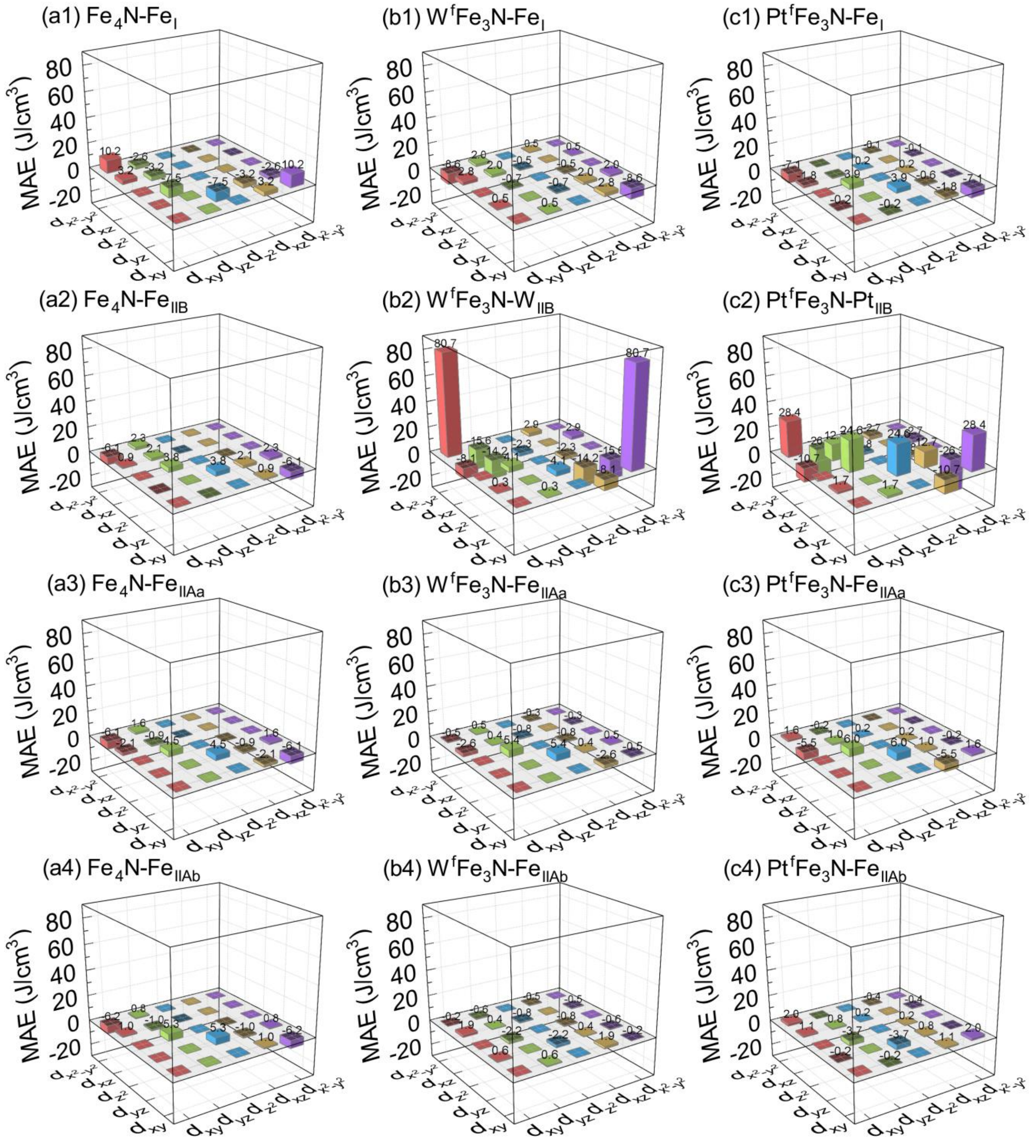

Figure S19 The orbital-resolved MAE of (a1-a4) Fe_4N, (b1-b4) W^fFe_3N, and (c1-c4) Pt^fFe_3N. The orbital-resolved MAE of (a1-c1) Fe_I, (a2-c2) Fe_{IIB}, (a3-c3) Fe_{IIAa}, and (a4-c4) Fe_{IIAb} sites.

S22. The orbital-resolved MAE of Fe_4N and M_3Fe^fN (M =W and Pt)

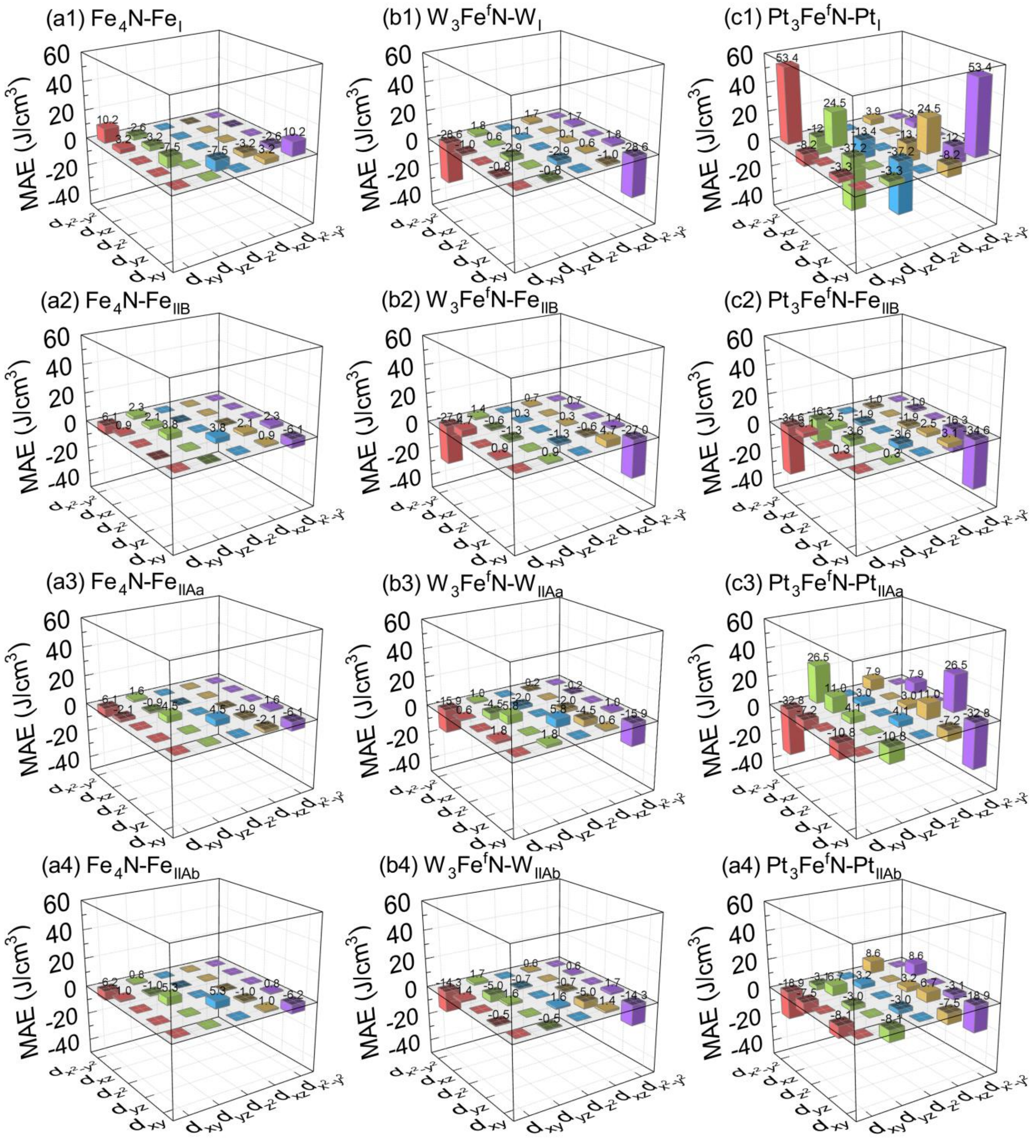

Figure S20 The orbital-resolved MAE of (a1-a4) Fe_4N, (b1-b4) W_3Fe^fN, and (c1-c4) Pt_3Fe^fN. The orbital-resolved MAE of (a1-c1) Fe_I, (a2-c2) Fe_{IIB}, (a3-c3) Fe_{IIAa}, and (a4-c4) Fe_{IIAb} sites.

S23. The orbital-resolved MAE of Fe_4N and M^fFe_3N (M = V, Cu, Zn, and Y)

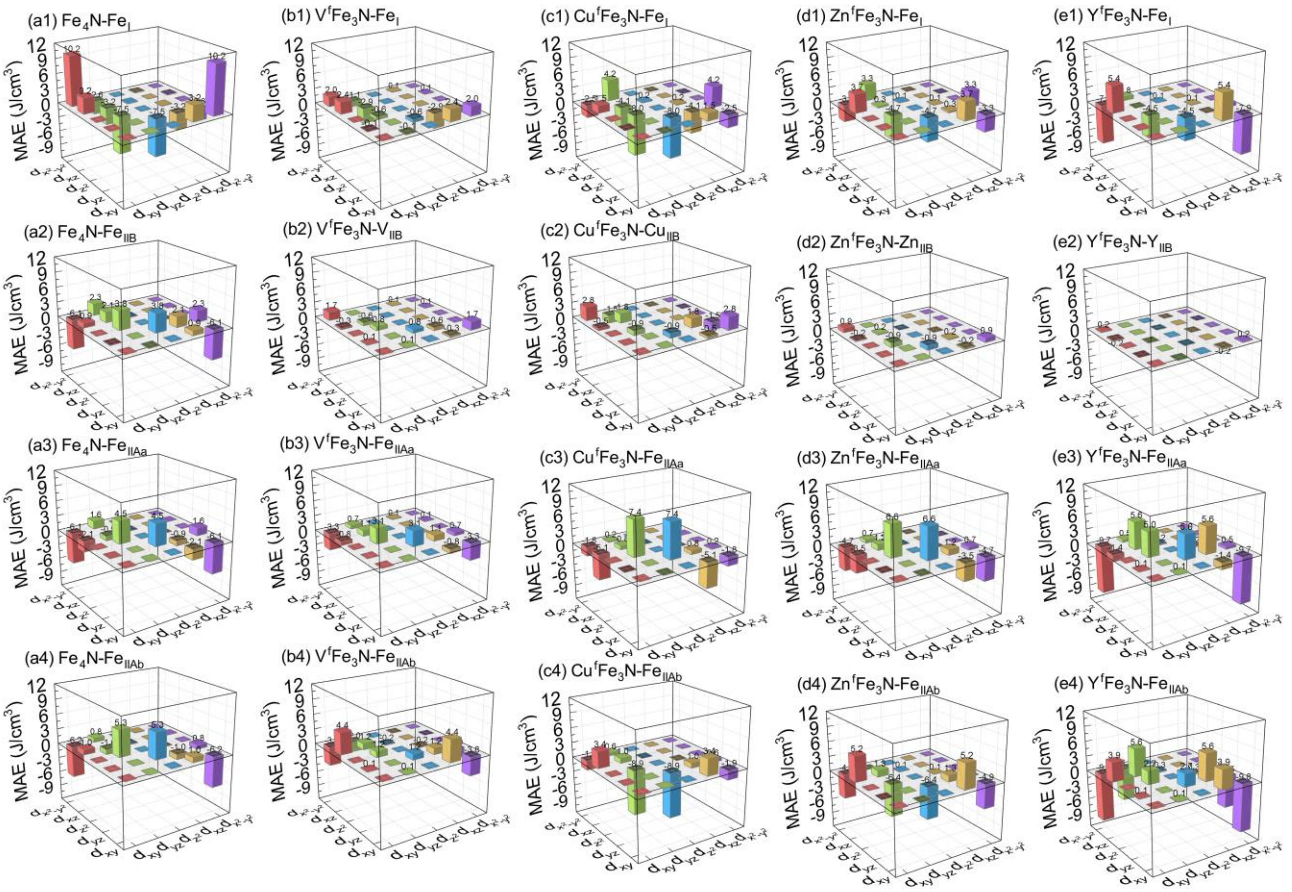

Figure S21 The orbital-resolved MAE of (a1-a4) Fe_4N, (b1-b4) V^fFe_3N, (c1-c4) Cu^fFe_3N, (d1-d4) Zn^fFe_3N, and (e1-e4) Y^fFe_3N. The orbital-resolved MAE of (a1-e1) Fe_I, (a2-e2) $Fe_{IIB,}$ (a3-e3) Fe_{IIAa}, and (a4-e4) Fe_{IIAb} sites.

S24. The priority occupancy of *M*Fe3N

Table S3 The energy difference $\Delta E=E_{(M^{c}Fe_{3}N)}-E_{(M^{f}Fe_{3}N)}$, where $E_{(M^{c}Fe_{3}N)}$ represents the energy of $M^{c}Fe_{3}N$ with cubic structure, and $E_{(M^{f}Fe_{3}N)}$ represents the energy of $M^{f}Fe_{3}N$ with tetragonal structure.

Substitution element	$E_{(M^{c}Fe_{3}N)}$	$E_{(M^{f}Fe_{3}N)}$	$\Delta E=E_{(M^{c}Fe_{3}N)}-E_{(M^{f}Fe_{3}N)}$	Preferential occupancy site
Gd	-46.845632	-41.178468	-5.667164	$Gd^{c}Fe_{3}N$
Pt	-38.479763	-37.078104	-1.401659	$Pt^{c}Fe_{3}N$
Zn	-34.527096	-33.164175	-1.362921	$Zn^{c}Fe_{3}N$
Cu	-36.888784	-36.192724	-0.696060	$Cu^{c}Fe_{3}N$
Mn	-42.122090	-42.045820	-0.076269	$Mn^{c}Fe_{3}N$
Co	-40.209929	-40.264990	0.055063	$Co^{f}Fe_{3}N$
Y	-36.274933	-36.485999	0.211066	$Y^{f}Fe_{3}N$
W	-41.081847	-41.536768	0.454921	$W^{f}Fe_{3}N$
Cr	-42.386732	-42.943333	0.556601	$Cr^{f}Fe_{3}N$
V	-42.431843	-43.040928	0.609085	$V^{f}Fe_{3}N$

The energy difference $\Delta E = E(M^{c}Fe_{3}N)-E(M^{f}Fe_{3}N)$, where $E(M^{c}Fe_{3}N)$ represents the energy of $M^{c}Fe_{3}N$ with cubic structure, and $E(M^{f}Fe_{3}N)$ represents the energy of $M^{f}Fe_{3}N$ with tetragonal structure. When $\Delta E < 0$, the element *M* tends to replace Fe_{I}, showing space group of *Pm*-3*m*. When $\Delta E > 0$, the element *M* tends to replace Fe_{IIB}, showing space group of *P*4/*mmm*.

S25. The priority occupancy of M_3FeN

Table S4 The energy difference $\Delta E=E_{(M_3Fe^cN)}-E_{(M_3Fe^fN)}$, where $E_{(M_3Fe^cN)}$ represents the energy of M_3Fe^cN with cubic structure, and $E_{(M_3Fe^fN)}$ represents the energy of M_3Fe^fN with tetragonal structure. When $\Delta E < 0$, the element M tends to replace Fe_{IIB} and Fe_{IIA}, showing space group of *Pm*-3*m*. When $\Delta E > 0$, the element M tends to replace Fe_{IIA} and Fe_I, showing space group of *P*4/*mmm*.

Substitution element	$E_{(M_3Fe^cN)}$	$E_{(M_3Fe^fN)}$	$\Delta E=E_{(M_3Fe^cN)}-E_{(M_3Fe^fN)}$	Preferential occupancy site
Y	-30.514946	-28.535864	-1.979082	Y_3Fe^cN
Gd	-60.553204	-59.635418	-0.917786	Gd_3Fe^cN
V	-45.925756	-45.449720	-0.476036	V_3Fe^cN
Co	-37.674500	-37.592495	-0.082005	Co_3Fe^cN
Cr	-45.801819	-45.725603	-0.076216	Cr_3Fe^cN
Mn	-43.859310	-44.229587	0.370276	Mn_3Fe^fN
W	-41.509129	-42.308742	0.799613	W_3Fe^fN
Pt	-27.385084	-28.933959	1.548875	Pt_3Fe^fN
Cu	-25.067883	-26.830467	1.762584	Cu_3Fe^fN
Zn	-16.692228	-18.478715	1.786487	Zn_3Fe^fN

The energy difference $\Delta E=E(M_3Fe^cN)-E(M_3Fe^fN)$, where $E(M_3Fe^cN)$ represents the energy of M_3Fe^cN with cubic structure, and $E(M_3Fe^fN)$ represents the energy of M_3Fe^fN with tetragonal structure. When $\Delta E < 0$, the element M tends to replace Fe_{IIB} and Fe_{IIA}, showing space group of *Pm*-3*m*. When $\Delta E > 0$, the element M tends to replace Fe_{IIA} and Fe_I, showing space group of *P*4/*mmm*.

S26. The phonopy of M_xFe$_{4-x}$N (M = V, Cr, Mn, Co, and Cu)

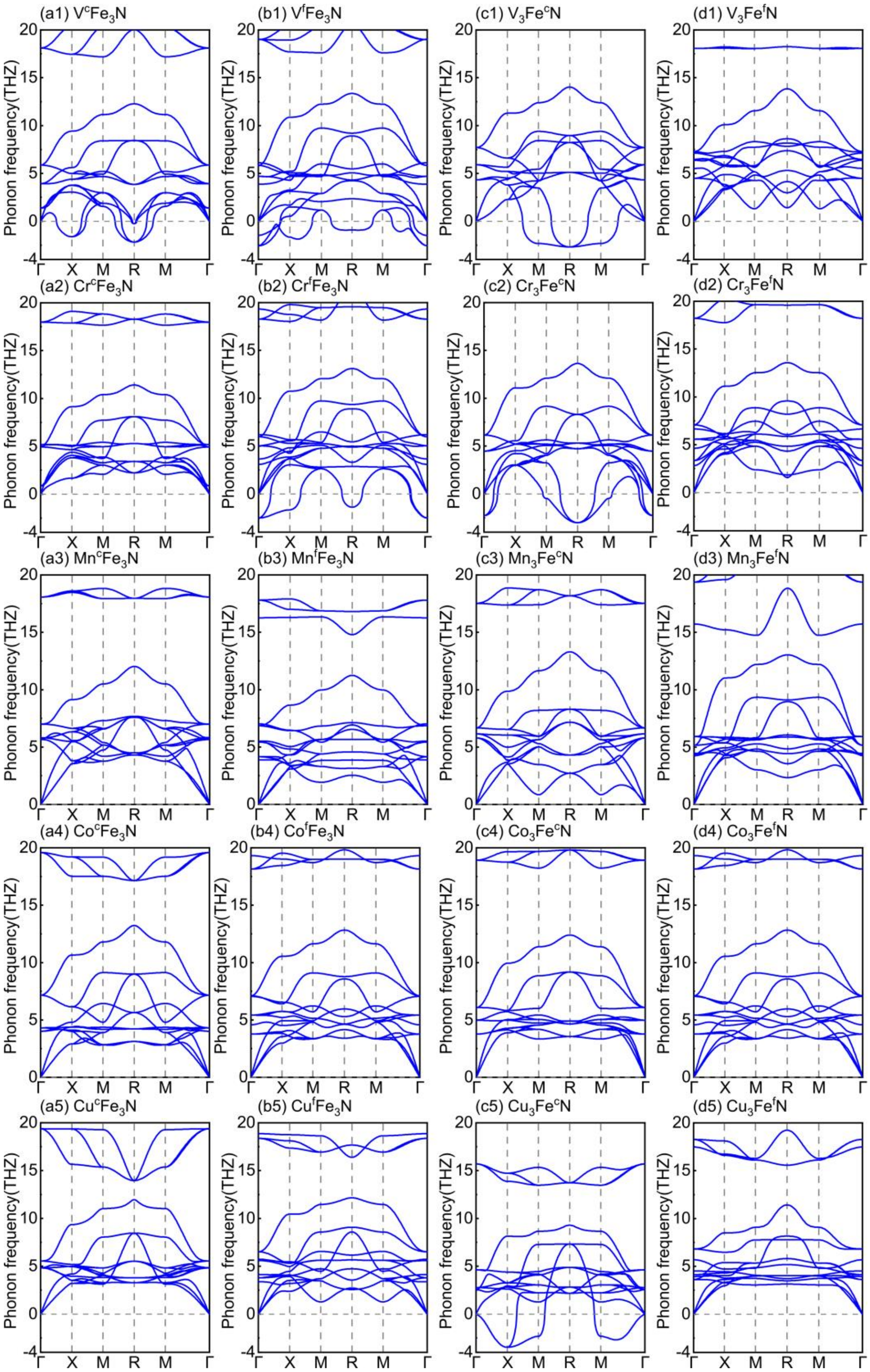

Figure S22 The phonopy of (a1-d1) V$_x$Fe$_{4-x}$N, (a2-d2) Cr$_x$Fe$_{4-x}$N, (a3-d3) Mn$_x$Fe$_{4-x}$N, (a4-d4), Co$_x$Fe$_{4-x}$N, and (a5-d5) Cu$_x$Fe$_{4-x}$N (x = 1 or 3).

S27. The phonopy of M_xFe$_{4\text{-}x}$N (M = V, Cr, Mn, Co, and Cu)

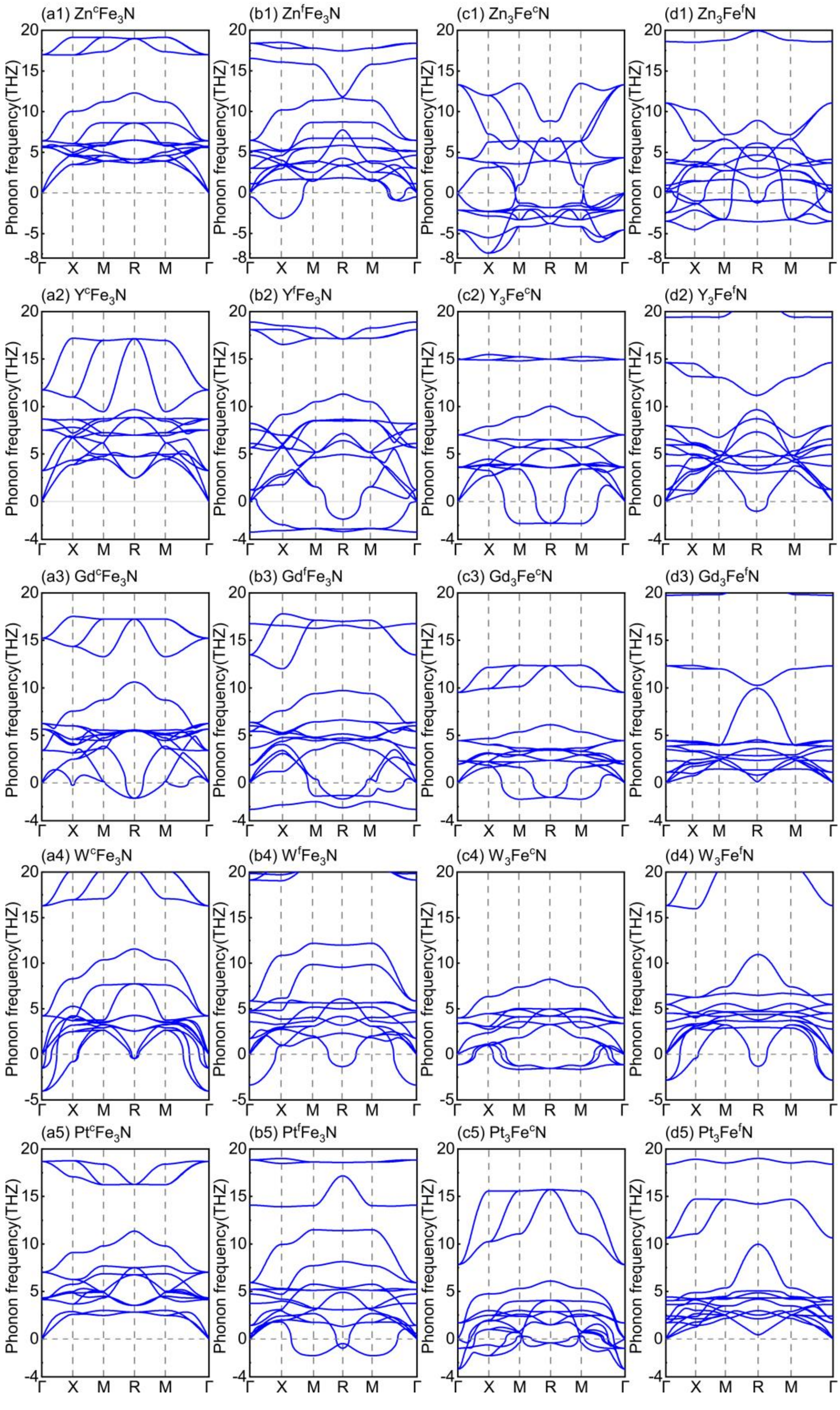

Figure S23 The phonopy of (a1-d1) Zn$_x$Fe$_{4\text{-}x}$N, (a2-d2) Y$_x$Fe$_{4\text{-}x}$N, (a3-d3) Gd$_x$Fe$_{4\text{-}x}$N, (a4-d4) W$_x$Fe$_{4\text{-}x}$N, and (a5-d5) Pt$_x$Fe$_{4\text{-}x}$N (x = 1 or 3).